Evidence of various mechanisms of Cd sequestration in the hyperaccumalator Arabidopsis halleri, the non accumulator Arabidopsis lyrata and their progenies by combined synchrotron-based techniques

M.-P. Isaure, Stéphanie Huguet, Claire-Lise Meyer, Hiram Castillo-Michel, Denis Testemale, Delphine D. Vantelon, Pierre Saumitou-Laprade, Nathalie Verbruggen, Geraldine Sarret

Journal of Experimental Botany, Vol. 66, No. 11 pp. 3201–3214, 2015
doi:10.1093/jxb/erv131 Advance Access publication 6 April 2015

RESEARCH PAPER

Evidence of various mechanisms of Cd sequestration in the hyperaccumulator *Arabidopsis halleri*, the non-accumulator *Arabidopsis lyrata*, and their progenies by combined synchrotron-based techniques

Marie-Pierre Isaure[1,*], Stéphanie Huguet[1], Claire-Lise Meyer[2], Hiram Castillo-Michel[3], Denis Testemale[4,5], Delphine Vantelon[6], Pierre Saumitou-Laprade[7], Nathalie Verbruggen[2,†] and Géraldine Sarret[8,†]

[1] Laboratoire de Chimie Analytique Bio-Inorganique et Environnement, Institut des sciences analytiques et de physico-chimie pour l'environnement et les matériaux (LCABIE/IPREM-UMR 5254), Université de Pau et des Pays de l'Adour and CNRS, Hélioparc, 2 Av. Pierre Angot, 64053 PAU Cedex 9, France
[2] Laboratoire de Physiologie et de Génétique Moléculaire des Plantes (LPGMP), Université Libre de Bruxelles, Campus Plaine-ULB, CP 242, Bd du Triomphe, B-1050 Brussels, Belgium
[3] European Synchrotron Radiation Facility (ESRF), ID21 Beamline, BP 220, 38043 Grenoble, France
[4] Université Grenoble Alpes, Institut Néel, 38000 Grenoble, France
[5] CNRS, Institut Néel, 38042 Grenoble France
[6] SOLEIL Synchrotron, LUCIA Beamline, BP48, 91192 Gif sur Yvette, France
[7] Laboratoire de Génétique et Evolution des Populations Végétales (GEPV-UMR 8198), Université des Sciences et Technologies de Lille and CNRS- Lille 1, 59655 Villeneuve d'Ascq Cedex, France
[8] Institut des Sciences de la Terre (ISTerre), Université Joseph Fourier and CNRS, BP 53, 38041 Grenoble Cedex 9, France

* To whom correspondence should be addressed. E-mail: marie-pierre.isaure@univ-pau.fr
† These authors contributed equally to this work.

Received 13 December 2014; Revised 16 February 2015; Accepted 26 February 2015

Abstract

***Arabidopsis halleri* is a model plant for Zn and Cd hyperaccumulation. The objective of this study was to determine the relationship between the chemical forms of Cd, its distribution in leaves, and Cd accumulation and tolerance. An interspecific cross was carried out between *A. halleri* and the non-tolerant and non-hyperaccumulating relative *A. lyrata* providing progenies segregating for Cd tolerance and accumulation. Cd speciation and distribution were investigated using X-ray absorption spectroscopy and microfocused X-ray fluorescence. In *A. lyrata* and non-tolerant progenies, Cd was coordinated by S atoms only or with a small contribution of O groups. Interestingly, the proportion of O ligands increased in *A. halleri* and tolerant progenies, and they were predominant in most of them, while S ligands were still present. Therefore, the binding of Cd with O ligands was associated with Cd tolerance. In *A. halleri*, Cd was mainly located in the xylem, phloem, and mesophyll tissue, suggesting a reallocation process for Cd within the plant. The distribution of the metal at the cell level was further discussed. In *A. lyrata*, the vascular bundles were also Cd enriched, but the epidermis was richer in Cd as compared with the mesophyll. Cd was identified in trichomes of both species. This work demonstrated that both Cd speciation and localization were related to the tolerance character of the plant.**

Key words: *Arabidopsis halleri*, backcross, cadmium, hyperaccumulation, μXRF, XAS.

Introduction

Cadmium (Cd) is one of the most toxic metals for biota, and no beneficial activity has been pointed out except in marine diatoms where it can replace zinc (Zn) in a specific isoform of carbonic anhydrase (Lane and Morel, 2000). The metal has been spread in the environment by human activity and in particular mining, ore treatment, and application of phosphate fertilizers (McLaughlin and Singh, 1999). Consequently some soils are contaminated and biota are exposed to Cd toxicity with the risk of metal transfer in the food chain via plants and water. *Itai-itai* disease, which concerned Japanese people contaminated by Cd from rice grown on mining soils, is one of the most patent examples of this environmental and health issue (Koji *et al.*, 1983).

Some higher plants can accumulate Cd with concentrations >100 μg g^{-1} dry weight (DW) in the shoots (for plants collected in their natural habitat), which is the threshold value for Cd hyperaccumulators (Baker and Brooks, 1989). To date, nine Cd hyperaccumulators have been identified. Four of them belong to the Brassicaceae familly: *Noccaea caerulescens* (previously *Thlaspi caerulescens*; Baker *et al.*, 1994), *Noccaea praecox* (previously *Thlaspi praecox*; Vogel-Mikuš *et al.*, 2008a), *Arabidopsis halleri* (Bert et al., 2002, 2003), and *Arabis paniculata* (Tang *et al.*, 2009a). Others come from various families and include *Picris divaricata* (Tang *et al.*, 2009b), *Sedum alfredii* (Yang *et al.*, 2006), *Phytolacca americana* (Liu *et al.*, 2010), *Potentilla griffithii* (Wang *et al.*, 2009), and *Viola boashanensis* (Liu *et al.*, 2004). These Cd hyperaccumulators also hyperaccumulate Zn, suggesting that Cd and Zn hyperaccumulations rely, at least partially, on common genetic determinants (Verbruggen *et al.*, 2009; Willems *et al.*, 2010).

Hyperaccumulation is characterized by a particular homeostasis network requiring enhanced root metal uptake, increased xylem loading and translocation from roots to shoots, followed by unloading in the shoots and specific sequestration and complexation (Verbruggen *et al.*, 2009; Krämer, 2010; Leitenmaier and Küpper, 2011). High expression of the *Heavy Metal ATPase4* (*HMA4*) gene was shown to be necessary for Zn and Cd hypertolerance and hyperaccumulation in *A. halleri* (Courbot *et al.*, 2007; Willems et al., 2007, 2010; Hanikenne *et al.*, 2008). *HMA4* encodes a P-type ATPase that acts as a plasma membrane pump loading Zn and Cd into the xylem. A high transcript level was also reported in *N. caerulescens* and was explained, as for *A. halleri*, by genomic copy number expansion and *cis*-activation (Hanikenne *et al.*, 2008; Ó Lochlainn *et al.*, 2011; Craciun *et al.*, 2012). The *Metal Transport Protein 1* gene (*MTP1*) coding for a Zn^{2+}/H^{+} antiporter is highly expressed in *A. halleri* (Assuncao *et al.*, 2001; Becher *et al.*, 2004; Dräger *et al.*, 2004; Shahzad *et al.*, 2010) and *N. caerulescens* (Assuncao *et al.*, 2001) due to a higher number of gene copies than in non-tolerant and non-accumulator relatives. *MTP1* expression was shown to increase shoot Zn concentrations when ectopically overexpressed in *Arabidopsis thaliana*, suggesting a key role in metal hyperaccumulation, but *MTP1* does not seem to transport Cd in such a clear way (Küpper and Kochian, 2010). Other genes have been proposed to participate in the complex process of Cd hyperaccumulation, including *ZIP* transporter genes (*ZRT*, *IRT-like Proteins*) for the absorption of Cd from soils into roots via Zn transporters, *AhNAS2* (*Nicotianamine Synthase 2*) for the root to shoot translocation, and *NcHMA3* transporter for the vacuolar sequestration in shoots (Verbruggen *et al.*, 2009; Krämer, 2010; Clemens *et al.*, 2013, and references herein).

Metal complexation in leaves is a way to cope with metal toxicity. The role of molecules containing sulphydryl groups such as glutathione, and phytochelatins, in Cd tolerance has been reported for normal tolerant plants but not in hyperaccumulators (Clemens, 2001; Cobbett and Goldsbrough, 2002; Clemens and Simm, 2003; Park *et al.*, 2012; Song *et al.*, 2013). However there is a role for glutathione in hyperaccumulation, which is probably related to its antioxidant activity (Verbruggen *et al.*, 2009) it is admitted that Cd hypertolerance is not related to enhanced phytochelatin synthesis or sequestration by phytochelatins (Ebbs *et al.*, 2002; Schat *et al.*, 2002; Sun *et al.*, 2007; Meyer and Verbruggen, 2012). Accordingly, the proportion of Cd co-ordinated by sulphur atoms is minor in shoots of hyperaccumulators such as *N. caerulescens* (Küpper *et al.*, 2004; Ueno *et al.*, 2005), *N. praecox* (Vogel-Mikuš *et al.*, 2010; Koren *et al.*, 2013), and *A. halleri* (Huguet *et al.*, 2012), and the main proportion of Cd is coordinated by oxygen atoms probably provided by organic acids (Küpper *et al.*, 2004; Ueno *et al.*, 2005; Tian *et al.*, 2011; Huguet *et al.*, 2012). Only a few studies reported major Cd–S complexes. It was observed for the *N. caerulescens* Ganges ecotype in contrast to the Prayon ecotype (Ebbs *et al.*, 2009). In that experiment, the Ganges ecotype was exposed to 100 μM Cd during 4 weeks, while the same concentration was applied during 6 months in the study of Küpper et al. (2004). This comparison suggests that the duration of exposure may play a role in Cd detoxification processes. Küpper et al. (2004) also demonstrated that Cd chemical forms varied with the age of leaves, with a lower proportion of Cd–S complexes in senescent leaves than in young and mature leaves of *N. caerulescens*.

Compartmentalization is another key process to cope with metal toxicity, by limiting metal interactions with metabolically active cells or with metabolically active compartments within the cell. However, Cd concentration was found to be higher in mesophyll tissue than in epidermis in *A. halleri* (Küpper *et al.*, 2000) and *S. alfredii* (Tian *et al.*, 2011). Although the reverse was found for *N. caerulescens* (Cosio *et al.*, 2005; Ma *et al.*, 2005), *N. praecox* (Vogel-Mikuš *et al.*, 2008a, b; Koren *et al.*, 2013), and for the non-hyperaccumulator *Silene vulgaris* (Chardonnens *et al.*, 1998), mesophyll accounts for the major storage site when considering the volume of the mesophyll in comparison with that of the epidermis. Some studies also reported that Cd was preferentially accumulated in younger leaves of *N. caerulescens* (Perronnet *et al.*, 2003) and *Brassica juncea* (Salt *et al.*, 1995), while Cosio *et al.* (2005) demonstrated preferential accumulation in mature leaves of *N. caerulescens*, especially at the edges of the leaves. These contrasting results reported for *N. caerulescens* suggest that Cd allocation may depend on various

parameters such as Cd exposure, growth conditions, age of the plant, or genotype. For *A. halleri*, Huguet *et al.* (2012) observed an increased Cd enrichment at the edge of mature leaves with time.

At the cell level, Cd distribution is also controversial. Vacuolar sequestration would protect the cytoplasm against metal toxicity. Accordingly, Cd vacuolar localization was evidenced in *N. caerulescens* (Ma *et al.*, 2005; Wójcik *et al.*, 2005; Ebbs *et al.*, 2009), and high expression of *NcHMA3* allows storage of Cd in the vacuoles of the leaf cells (Ueno *et al.*, 2011). This distribution was also observed in *S. alfredii* (Tian *et al.*, 2011). However, in *N. praecox*, vacuolar sequestration was obtained upon application of $CdCl_2$, while apoplastic localization was observed after $CdSO_4$ treatment (Koren *et al.*, 2013). In *N. caerulescens* from the Ganges and Prayon ecotypes, up to 35% of Cd was found in the cell wall from the mesophyll and epidermis (Cosio *et al.*, 2005), and association of Cd with the cell wall in addition to vacuoles was also observed in the non-accumulator *Brassica napus* (Carrier *et al.*, 2003). All these results pinpoint that vacuolar compartmentalization may not be the only way for Cd detoxification. Compartmentalization of Cd in trichomes of *A. halleri* has been reported, although this pool is clearly not the main Cd storage site (Küpper *et al.*, 2000; Fukuda *et al.*, 2008; Huguet *et al.*, 2012). It was also observed for the non-hyperaccumulators *B. juncea* (Salt *et al.*, 1995) and *A. thaliana* (Isaure *et al.*, 2006).

Arabidopsis halleri is a pseudo-metallophyte, growing on both contaminated and non-contaminated sites. It is phylogenetically close to the model plant *A. thaliana* and is considered as a model to investigate metal tolerance and hyperaccumulation (Roosens *et al.*, 2008). Interspecific crosses between *A. halleri* and its non-tolerant and non-hyperaccumulating relative *Arabidopsis lyrata* ssp. *petraea* can be done to obtain progenies with various traits of Cd tolerance and accumulation in *A. halleri* (Macnair *et al.*, 1999; Bert *et al.*, 2003). Three loci were identified that control the segregation of Cd tolerance, explaining, respectively, 43, 24, and 16% of the phenotypic variance (Courbot *et al.*, 2007). The major quantitative trait locus (QTL) for Cd tolerance was shown to co-localize with the *HMA4* gene and with the QTL for Cd accumulation (Willems *et al.*, 2010). These progenies were also used to study the relationship between the localization, the chemical forms, and the Zn accumulation capacity of leaves (Sarret *et al.*, 2009). It was shown that the amount of Zn in octahedral coordination with organic acids and aqueous Zn ranged from 40% to 80% of total Zn in leaves, and that this pool increased with Zn accumulation. Zn contained in the leaf tissue (including the mesophyll and epidermis) in comparison with vascular tissues also increased with Zn accumulation. Taken together, all these results suggest that the hyperaccumulation is related to a high unloading from xylem to leaf tissue where the metal is mainly stored as Zn–organic acid complexes. As suggested in other studies on *A. halleri*, Zn could be stored in the leaf mesophyll (Küpper *et al.*, 2000; Zhao *et al.*, 2000), and at the cellular level in the vacuoles (Küpper *et al.*, 2000).

In the present work, the BC_1 progenies from interspecific crosses between *A. halleri* and *A. lyrata* segregating for Cd tolerance and accumulation were studied. The objective was to determine the relationship between Cd localization, speciation, and Cd accumulation and tolerance. Cd distribution was investigated in the parents and Cd speciation in the parents and progenies to clarify the link between the storage mechanisms in the leaves and tolerance and accumulation traits.The influence of Cd exposure time on Cd speciation in the parents was also investigated. Cd distribution was investigated using synchrotron micro X-ray fluorescence (μXRF) and Cd speciation by X-ray absorption near edge structure (XANES) and extended X-ray absorption fine structure (EXAFS) spectroscopy. These techniques are complementary to molecular biology approaches and offer the great advantage of causing minimal sample perturbation (Sarret *et al.*, 2013).

Materials and methods

Plant material

Arabidopsis halleri ssp. *halleri* originating from the metallicolous site of Auby, France (CH2.1 genotype), and *A. lyrata* ssp. *petraea* originating from a non-contaminated site in the Czech Republic were selected. They were crossed to provide the F_1 progeny, which were backcrossed with the *A. lyrata* species to produce various backcross progenies (Courbot *et al.* 2007). In both crosses, *A. lyrata* was used as the mother.

Progenies were characterized for Cd tolerance according to the sequential test of Courbot *et al.* (2007). Briefly, at least three cuttings of each genotype were transferred in 4 litre vessels filled with a modified Murashige and Skoog solution (Supplementary Table S1 available at *JXB* online). To minimize local environmental effects, seedlings were randomly distributed in the vessels and the vessels moved around once a week during a change of solution. After 3 weeks, plants were transferred weekly to sequentially increasing concentrations of Cd (from 10 μM to 250 μM $CdSO_4$). At the end of each week, the roots of each plant were gently dried with paper and the whole plant was weighed. Tolerance was determined as the lowest concentration at which no increase in biomass was observed (EC_{100}, effective concentration for 100% growth inhibition). Finally, genotypes showing contrasting phenotypes were selected for this study. Individuals displaying an EC_{100} similar to *A. lyrata* (i.e. <50 μM) were considered 'non-tolerant' whereas individuals with an EC_{100} >100 μM were considered 'tolerant' (Table 1). At least three cuttings of the BC_1 parents and of the selected progenies (n=10) were grown on sand during 5 weeks for rooting, transferred into hydroponic cultures during 3 weeks without Cd, and finally exposed to 10 μM $CdSO_4$ for 1 week. In parallel, BC_1 parents were also exposed to 10 μM $CdSO_4$ for 3 weeks. Note that the sulphate concentration added with $CdSO_4$ was low compared with the sulphate concentration in the Murashige and Skoog medium and was not expected to influence Cd speciation in the plants. A summary of the analyses is provided in Supplementary Table S2.

For chemical analyses, a minimum of three leaves per plant were harvested, pooled with individuals from the same genotype, washed in ultrapure water, dried at 65 °C, and ground. The others leaves were washed and gently dried.

For μXRF and μXANES measurements, leaves (not the youngest or the oldest) were set in a cryo-embedding OCT compound (Tissue Tek®) and rapidly plunged into liquid nitrogen. They were kept at –80 °C until preparation of cryo-sections. Prior to measurements, 30 μm thick cryo-sections were prepared using a cryo-microtome, deposited in between cooled Ultralene film (SPEX), transferred to the microscope in their frozen hydrated state, and kept frozen during

Table 1. *Tolerance phenotypes and Cd concentrations in the parents* A. halleri *and* A. lyrata*, and in BC$_1$ progenies*

	Phenotype	Cd µg g^{-1} dry weight[a]
A. halleri 1 week Cd	Tolerant	609±40
A. halleri 3 weeks Cd		818±14
A. lyrata 1 week Cd	Sensitive	175±4
A. lyrata 3 weeks Cd		249±6
F_1 1 week Cd	Tolerant	300±5
BC $_{57\,22}$ 1 week Cd	Tolerant (133)	68±2
BC $_{55\,05}$ 1 week Cd	Tolerant (183)	255±5
BC $_{54\,11}$ 1 week Cd	Tolerant (116)	89±2
BC_{95} 1 week Cd	Tolerant (150)	228±1
BC_{93} 1 week Cd	Tolerant (125)	271±4
Average tolerant ±SD		201.8±98.5
BC $_{58\,09}$ 1 week Cd	Sensitive (50)	117±3
BC $_{57\,02}$ 1 week Cd	Sensitive (25)	125±2
BC $_{62\,27}$ 1 week Cd	Sensitive (50)	235±6
BC $_{54\,19}$ 1 week Cd	Sensitive (37.5)	44±1
BC_{121} 1 week Cd	Sensitive (25)	65±1
Average non-tolerant ±SD		117.2±74.2

Values in parentheses represent EC_{100} values, i.e. the lowest concentration at which no increase in biomass was observed.
[a] Standard deviation was calculated from five ICP-MS measurements of the sample (individual plants were pooled), except for *A. halleri* where three replicates were digested and measured.

analysis. A minimum of three leaves were observed by µXRF. For bulk XANES and EXAFS measurements, leaves from replicates were pooled, ground in nitrogen liquid, prepared as frozen pressed pellets, and kept frozen during analysis. The cryo-sample preparation minimizes the sample perturbation, limiting the redistribution of soluble species, and the chemical change of metal complexes with low stability (Sarret *et al.*, 2013). Moreover, synchrotron measurements at low temperature limit X-ray radiation damage, which could have a dramatic effect on biological samples.

Chemical analyses

Ground dried leaves were digested in 2.5 ml of 65% HNO_3 and 2.5 ml of 30% H_2O_2 during 3 h at 80 °C. Then the solution was filtered at 0.45 µm, diluted to 2% HNO_3, and elemental concentrations were measured by inductively coupled plasma mass spectrometry (Agilent 7500). The non-parametric statistical test (Mann–Withney) was performed to calculate the significance of differences between tolerant and non-tolerant progenies.

Synchrotron measurements

µXRF and Cd L_{III}-edge µXANES were conducted on the ID21 scanning X-ray microscope at the European Synchrotron Radiation Facility (ESRF, Grenoble, France) and for the trichome study on beamline LUCIA at the SOLEIL synchrotron (Saclay, France), with lateral spatial resolution of 0.73 µm (H)×0.25 µm (V) and 3.5 µm (H)×3.2 µm (V), respectively (see the Supplementary data at *JXB* online). All measurements were performed at 100K using a liquid nitrogen cryostat.

Cd L_{III}-edge µXANES spectra were collected with the same lateral resolution as µXRF, in the energy range 3520–3590 eV. Normalized XANES spectra were then compared with the spectra of previously recorded Cd model compounds (Isaure et al., 2006, 2010; Huguet *et al.*, 2012). A fingerprint approach was used to simulate the unknown spectra by linear combination fits (LCFs) of Cd references as described in Isaure *et al.* (2006). The quality of the fit was estimated by the normalized sum-squares residual *NSS* parameter ($NSS=\Sigma\,[\mu_{exp}-\mu_{fit}]^2/\Sigma[\mu_{exp}]^2\times100$).

Cd K-edge bulk XANES and EXAFS spectra were collected on the FAME beamline at ESRF (see the Supporting data at *JXB* online). Frozen pellets of leaves were transferred into a helium cryostat operating at 10K for analysis. The LCF approach was used to analyse the XANES spectra in the 26 680–26 865 eV range. The quality of the fits was estimated using the *NSS* parameter as defined for Cd L_{III}-edge. EXAFS spectra were collected when the Cd concentrations were sufficiently high. The extraction of EXAFS signal was performed according to standard methods. The k^3-weighted EXAFS spectra were least-squares fitted over a k range of 3.0–11 Å^{-1}. The quality of the fit was estimated by the *NSS* parameter where $NSS=\Sigma\,[k^3\,\chi_{exp}-k^3\,\chi_{fit}]^2/\Sigma\,[k^3\,\chi_{exp}]^2\times100$). The standard spectra used for Cd K-edge XANES and EXAFS LCFs (including Cd–cell wall) were collected previously (Huguet *et al.*, 2012).

For XANES and EXAFS, LCFs with one, two, and three components were tested and the fit with n+1 components was retained if the *NSS* value was decreased by >20% compared with the fit with n components. The uncertainty of the proportion of each compound was estimated to 10%.

For EXAFS spectra, the structural parameters were determined by shell simulations using ARTEMIS software (Ravel and Newville, 2005). Phase and amplitude functions were calculated by FEFF 6.0 from Cd compounds found in the ICSD database. For Cd model compounds, EXAFS spectra were Fourier transformed over a k range of 3.5–11.5 Å^{-1}, while the noisier plant spectra were transformed from a shorter range (see the Results below). The contribution of the first shell was simulated in R space, either with O atoms only, or with O and S atoms. The second shell was simulated for some Cd model compounds exhibiting a pronounced second shell contribution.

Results

Cd accumulation in plants

The parents and progenies used for this study are presented in Table 1. Although no biochemical marker of toxicity was studied, the number of leaves after exposure to 10 µM Cd was examined. For *A. halleri*, the number increased between 1 and 3 weeks treatment, whilst for *A. lyrata* it did not increase. The number of leaves was lower for the sensitive progenies than for the tolerant ones. The plants were tested for their Cd accumulation capacities after 1 week (plus 3 weeks for the parents) exposure to Cd. Cd concentrations were higher in the hyperaccumulating parent than in the non-accumulator parent, regardless of the exposure time (609 µg g^{-1} and 818 µg g^{-1} after 1 and 3 weeks, respectively, for *A. halleri*, and 175 µg g^{-1} and 249 µg g^{-1} for *A. lyrata*) (Table 1). The ratio between *A. halleri* and *A. lyrata* (3.5 and 3.2 for 1 and 3 weeks, respectively) is in agreement with the ratio of 3.9 measured for plants grown for 6 weeks in compost amended with 10 mg Cd kg^{-1} fresh soil (Willems *et al.*, 2010). Cd concentrations were always lower in tolerant progenies than in *A. halleri* and were variable, ranging from 68 µg g^{-1} to 300 µg g^{-1} shoot DW, indicating contrasting accumulation of the genotypes.

For sensitive progenies, heterogeneity of Cd concentrations between genotypes was also observed, with values ranging from 44 µg g^{-1} to 235 µg g^{-1} shoot DW. The average Cd concentration of tolerant progenies was not statistically different from that of sensitive progenies (P=0.309; Mann–Whitney exact test). Note that accumulation was not correlated with Cd tolerance (Spearman correlation, r=0.513, P=0.163, n=10).

Cd chemical forms by bulk Cd K-edge XAS

Cd K-edge XANES (parents and progenies)

The Cd species in leaves were investigated by Cd K-edge XANES. Spectra were first compared with Cd reference spectra (Fig. 1). When the first Cd coordination sphere is composed of S atoms, for example Cd–cysteine, Cd–GSH (Cd complexed with glutathione), and Cd–PC_2 (Cd complexed with phytochelatin 2), the white line (i.e. the intense absorption peak after the edge; arrow in Fig. 1) is much reduced compared with a first sphere constituted of O or N atoms. The oscillations for the S-containing ligands are also shifted to higher energy values than those for O ligands (a and b in Fig. 1). Examination of the plant samples showed that the spectrum of *A. halleri* treated for 3 weeks had the white line and frequency typical of an O binding molecule whereas these matched S binding molecules more in *A. lyrata* treated for 3 weeks. When decreasing the exposure time to 1 week, the white line intensity decreased for both *A. halleri* and *A. lyrata*, suggesting the increase of the proportion of S bonds with Cd. Using the fingerprint approach, after 1 week of Cd exposure, the spectra of *A. lyrata* and sensitive progenies (BC_{6227} and BC_{121}) were satisfactorily fitted with one component only, Cd–cysteine, Cd–GSH, or Cd–PC_2 (Fig. 1). A better spectral match was obtained for Cd–GSH and Cd–PC_2 in comparison with Cd–cysteine (Supplementary Fig. S1 at *JXB* online), but it is difficult to identify with certainty the nature of this binding thiol-containing molecule due to very small differences between spectra. Therefore, in the LCF results displayed in Fig. 2, a single 'Cd–S' species was defined, and it can be inferred that in sensitive plants, after 1 week exposure, Cd is coordinated by sulphur ligands. The complexation of Cd by the various sulphur donors is discussed further.

After 3 weeks of Cd exposure, the *A. lyrata* XANES spectrum was satisfactorily fitted with 69% Cd–GSH and 30% Cd–cellulose ($NSS=1.58\times10^{-2}$, Fig. 1; Supplementary Fig. S1 at *JXB* online). Note that percentages given in the text of Fig. 1 are not normalized, whereas they are in Fig. 2 for easier comparison. A good fit was also found with 70% Cd–GSH and 30% Cd–citrate, although the spectral agreement was slightly degraded ($NSS=2.04\times10^{-2}$; Supplementary Fig. S1). These results suggest that between 1 and 3 weeks of exposure, a minor part of Cd (30%) is transferred from S- to O-containing ligands, possibly carboxyl/hydroxyl groups provided by cell wall compounds (cellulose, hemicellulose, and pectin) and/or organic acids. As for Cd–S species, it is not possible to identify the exact nature of these O-containing ligands due to small variations between spectra, and they were defined as 'Cd–O' species in Fig. 2.

After 1 week of Cd exposure, a good fit of the *A. halleri* spectrum was obtained with 68% Cd–cellulose+29% Cd–GSH (Figs 1, 2; Supplementary Fig. S1 at *JXB* online). After 3 weeks, an increase in the proportion of O ligands was observed (83% Cd–cellulose+13% Cd–GSH; Figs 1, 2; Supplementary Fig. S1). Thus, the proportion of O ligands is clearly higher after 3 weeks than after 1 week of exposure.

The spectra of all the tolerant progenies (F_1, BC_{93}, BC_{95}, and $BC_{54\ 11}$) were correctly fitted with various combinations of Cd–cellulose and Cd–GSH with O ligands, ranging from 31% to 86% (Figs 1, 2).

Thus, tolerant plants from the backcross are characterized by a majority of Cd–O species, whereas sensitive plants are dominated by Cd–S species. There was no relationship between Cd accumulation and the proportion of Cd–S or Cd–O species.

*Cd K-edge EXAFS (*A. halleri*)*

Cd K-edge EXAFS spectra were recorded on *A. halleri* only since Cd in the other samples was not sufficiently concentrated. Plant spectra and some Cd model compounds together with their Fourier transforms (FTs) are displayed in Fig. 3. The frequency of oscillations for Cd–thiol complexes is higher than for Cd–O and N ligands, which is reflected by a clear shift of the first peak of the FT to higher R+ΔR values.

The *A. halleri* spectrum after 1 week of Cd exposure was very noisy, particularly after 7.5 $Å^{-1}$. Using LCF, it was reproduced with 55% Cd–cellulose+35% Cd–GSH (NSS=12.4) or 47% Cd–malate+43% Cd–GSH (NSS=13.4) (Fig. 3). After 3 weeks, good fits were obtained with 66% Cd–cellulose+18%

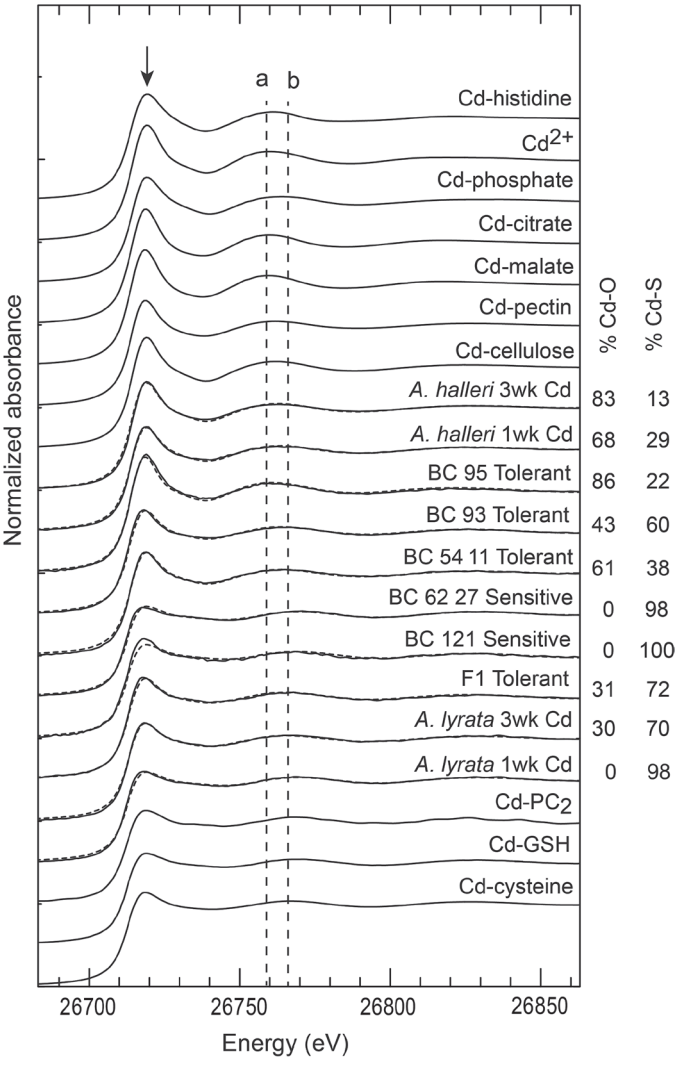

Fig. 1. Cd K-edge XANES spectra for Cd reference compounds, *A. halleri*, *A. lyrata*, and progenies after 1 week or 3 weeks exposure to 10 μM Cd (solid lines) with their linear combination fits (dashed lines). The proportions of the best fit were expressed in percentages ±10%.

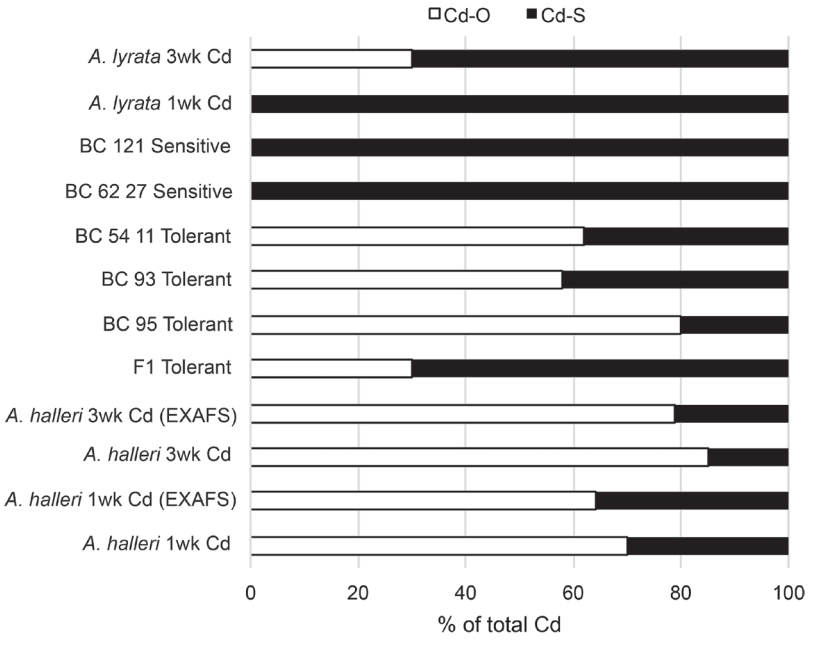

Fig. 2. Proportion of Cd species (in % mole fraction) obtained by XANES and EXAFS LCFs after normalization of the percentages to 100%. The uncertainty of the proportion of each compound was estimated to 10%.

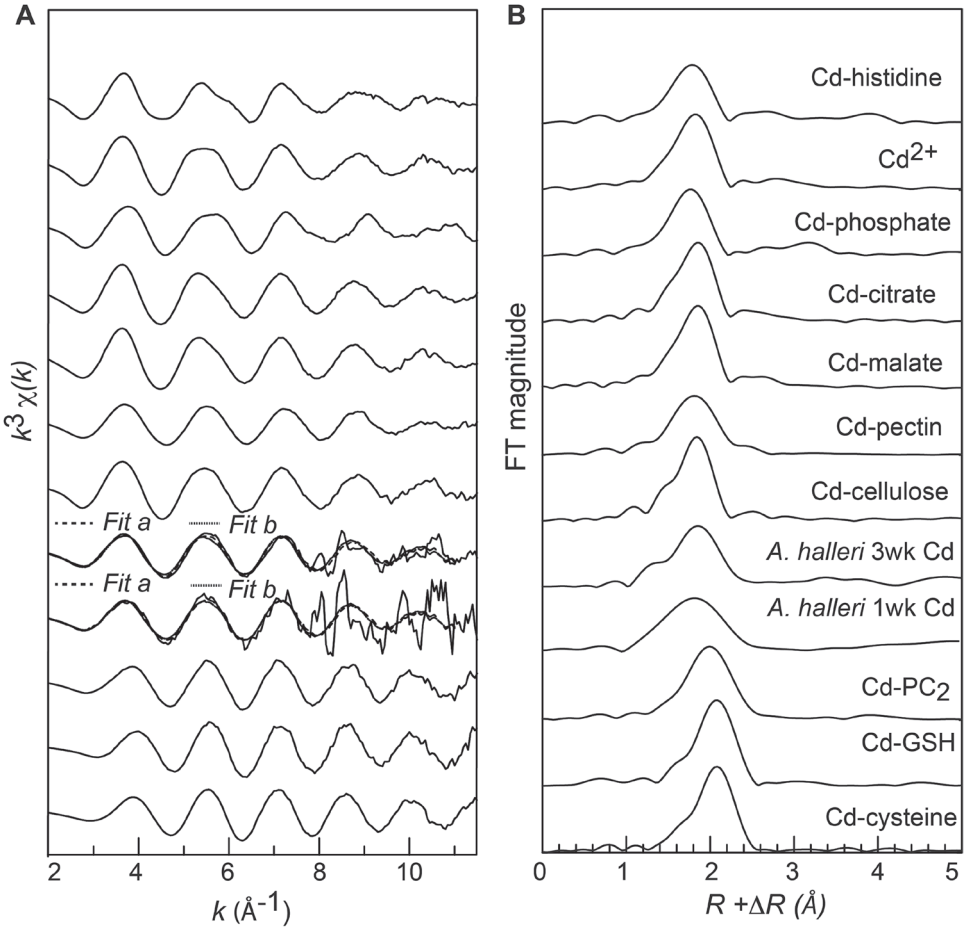

Fig. 3. Cd K-edge EXAFS spectra (A) and Fourier transforms (B) for Cd reference compounds and *A. halleri* leaves after 1 and 3 weeks of Cd exposure. Dashed and dotted lines represent linear combination fits: for *A. halleri* at 3 weeks Cd exposure, Fit a is 66% Cd–cellulose+18% Cd–GSH (*NSS*=17.0) and Fit b is 58% Cd–malate+23% Cd–GSH (*NSS*=20.7); for *A. halleri* at 1 week Cd exposure, Fit a is 55% Cd–cellulose+35% Cd–GSH (*NSS*=12.4) and Fit b is 47% Cd–malate+43% Cd–GSH (*NSS*=13.4).

Table 2. *Shell structural parameters obtained by shell fitting of the EXAFS spectra for* A. halleri *samples and some Cd model compounds*

	Shell	Atom	N	R (Å)	σ^2 (Å^2)	*NSS*
Cd–cellulose	First	O	7.0	2.31	0.007	0.068
	Second	C	2.7	3.23	0.012	
Cd–pectin	First	O	6.5	2.32	0.009	0.011
	Second	C	2.7	2.76	0.009	
Cd–malate	First	O	6.5	2.32	0.006	0.010
	Second	C	5.0	3.21	0.012	
Cd–cysteine	First	S	3.9	2.54	0.005	0.005
		O	0.7	2.27	0.005	
Cd–GSH	First	S	3.9	2.54	0.005	0.006
		O	0.7	2.26	0.005	
A. halleri 1 week Cd	First	O	5.5	2.32	0.008	0.242
	First	O	2.8	2.32	0.008	0.195
		S	2.4	2.52	0.008	
A. halleri 3 weeks Cd	First	O	5.4	2.32	0.008	0.048
	First	O	4.6	2.32	0.008	0.028
		S	0.9	2.52	0.008	

N, number of atoms; R, interatomic distance; σ^2, Debye Waller factor; $NSS = \Sigma\,[k^3\,\chi_{exp} - k^3\,\chi_{fit}]^2 / \Sigma\,[k^3\,\chi_{exp}]^2 \times 100$ with Fourier-filtered EXAFS signal. Experimental errors on N and R are estimated to 10% and 0.01 Å for the first shell, and 20% and 0.02 Å for the second shell. The first two shells were calculated for Cd–cellulose and Cd–malate, whilst the first shell was calculated for Cd–cysteine, Cd–GSH, and *A. halleri* samples.

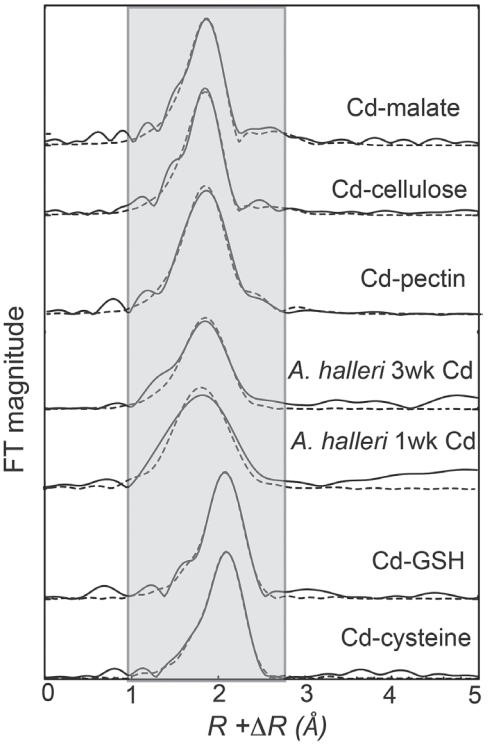

Fig. 4. Cd K-edge EXAFS Fourier transforms of some Cd–model compounds and *A. halleri* samples and their shell fittings (dotted lines). The fitted range is represented in grey.

Cd–GSH (*NSS*=17.0) and 58% Cd–malate+23% Cd–GSH (*NSS*=20.7). As for XANES, it was not possible to distinguish Cd–cell wall from Cd–organic acid complexes, thus O-containing species were classified as 'Cd–O' (Fig. 2).

EXAFS spectra were treated by shell fitting to obtain structural parameters (Table 2; Fig. 4). Cd–cellulose and Cd–malate showed similar structural parameters, indicating a 6-fold oxygen coordination with Cd–O distances of 2.31 and 2.32 ± 0.1 Å. A 4-fold coordination was found for Cd–cysteine and Cd–GSH. S atoms were identified as the binding atoms at 2.54 ± 0.1 Å, while a very small contribution of oxygen was found at 2.27 and 2.26 ± 0.1 Å, respectively. The contribution of the second shell was too low to be simulated.

The *A. halleri* EXAFS spectra are noisy and their FTs are not well resolved. This was particularly the case for the 1 week exposure spectrum, whose FT was extracted until 9.8 Å^{-1}, while the 3 weeks exposure FT was extracted from the spectrum until 10.1 Å^{-1}. Both FTs have an intense peak and weak contribution at higher distances. The *A. halleri* spectrum after 3 weeks of Cd exposure is slightly shifted to a lower distance compared with 1 week, meaning that the contribution of oxygen atoms in Cd coordination is higher (Fig. 3). First shell fits using O atoms only were significantly improved when considering both S and O ligands (Table 2; Fig. 4). Cd–O distances were the same for both exposure times (2.32 ± 0.1 Å) but the number of O atoms increased from 2.8 ± 10% after a 1 week exposure to 4.6 ± 10% after a 3 weeks exposure, while at the same time the number of S ligands at 2.52 ± 0.1 Å decreased from 2.4 ± 10% to 0.9 ± 10%. Thus, the O/S ratio increased from 1.2 to 5.1 between 1 week and 3 weeks Cd exposure.

Cd localization in the parent plants by µXRF

Arabidopsis halleri and *A. lyrata* after 3 weeks of Cd exposure were imaged using µXRF. In the leaves of the hyperaccumulator, Cd enrichments were observed in the vascular system including the central and secondary veins (Fig. 5A). In the midrib, the metal was found not only in the xylem (the sap itself cannot be distinguished from the vascular bundles), but also, and more intensely, in the phloem area. The presence in the phloem suggests that the metal could be re-allocated from leaves. The distribution of S and P in the vascular regions more or less matched that of Cd, with slight variations (e.g. Fig. 5A). Cd was also present in the mesophyll tissue. The edge of the leaf was more Cd enriched than the other parts of the leaf, as previously observed by Huguet *et al.* (2012) by autoradiography. The epidermal region presented in Fig. 5B showed no Cd accumulation in this tissue. At the cell level, the presence of P and S in the cell walls instead of the intracellular compartment for the section presented in Fig. 5A probably indicates some damage during freezing or sample manipulation. This artefact was more pronounced in the thicker parts of the leaf, and for larger cells. Figure 5C shows elemental maps of the mesophyll obtained on a smaller leaf, in which cells are better preserved, with S, P, and K in the intracellular compartment. Cd was found inside the cell and at the rim of the cell, as attested by the sum of µXRF spectra for the two regions (Fig. 5D). These data suggest a cell wall/apoplast localization in addition to the intracellular pool. More analyses on larger zones with intact cells should be done to confirm this observation.

In *A. lyrata* leaves, cadmium was located in the vascular system (Fig. 6A, B), probably in both xylem and phloem

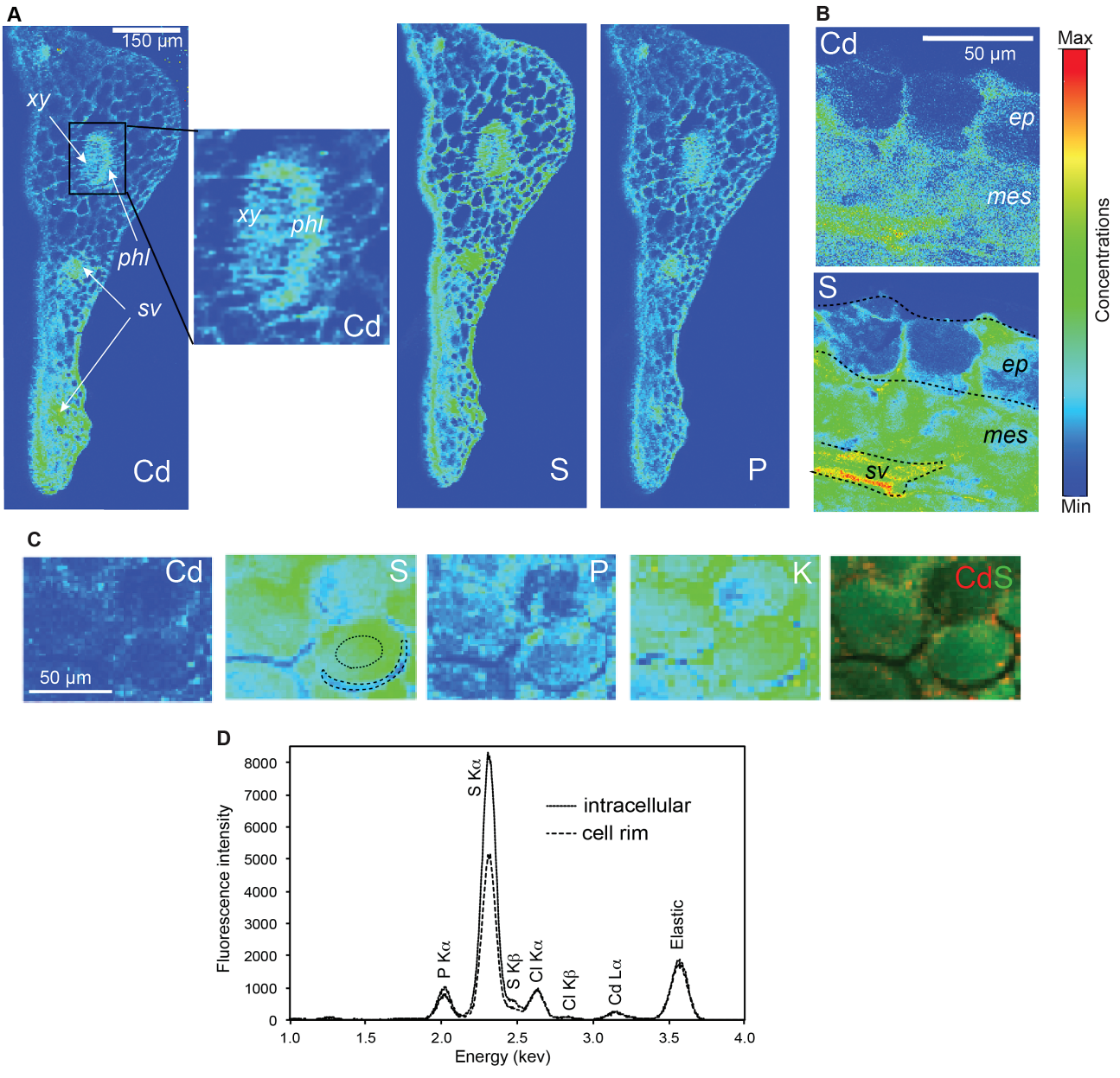

Fig. 5. Elemental µXRF maps (A–C) of cryo cross-sections of *Arabidopsis halleri* after 3 week Cd treatment (step size=3 µm, counting time=100 ms for A; step size=0.5 µm, counting time=600 ms for B; step size=2 µm, counting time=100 ms for C) with a zoom on the central vein for A (inset). On the maps in A, mesophyll cells in the thicker part of the leaf have lost their content. However, these maps clearly show enrichment in Cd in vascular tissues including the central vein [xylem (xy) and phloem (phl)] and secondary veins (sv), and at the edge of the leaf. On the maps in B, the epidermis (ep) seems depleted in Cd as compared with the mesophyll (mes). (C) Elemental distributions for well preserved cells, and a Cd and S bicolor. (D) XRF spectra extracted from map C (E=3570 eV) for the intracellular compartment (dotted area) and rim (dashed area) of a cell. (This figure is available in colour at *JXB* online.)

areas, and to a lesser extent in the epidermis and mesophyll cells. In comparison with the hyperaccumulator, the mesophyll was less enriched while the epidermis contained more Cd. The lateral resolution and the level of Cd were too low to evidence the cellular distribution. High local concentrations of Cd were observed at the half height of the trichomes of *A. halleri*, and this Cd spot was co-localized with a sharp change in Ca and P concentrations, which are enriched in the upper part (Fig. 7). An optical image of the trichome suggests a partition-like structure in this region, potentially an incursion of the cell wall, but its nature is not clear. The same Cd enrichment was observed for *A. lyrata* (not shown).

Cd chemical forms by Cd L_{III}-edge µXANES

µXANES spectra were collected on some points of *A. halleri* maps (Figs 5, 7) and *A. lyrata* maps (Figs 6, 8). The spectrum from the Cd hot spot in trichomes clearly showed the occurrence of the peak at 3539 eV typical of O ligands (Isaure *et al.*, 2006). The best fit was obtained with two components: 61% Cd–cell wall+30% Cd_{aq} (*NSS*=2.20 10^{-4}). Thus, in the trichome, Cd is bound to 100% O ligands. The collection of µXANES spectra in xylem, phloem, and epidermis was difficult due to the heterogeneity of the Cd enrichment at the submicrometre scale, and thus at the beam

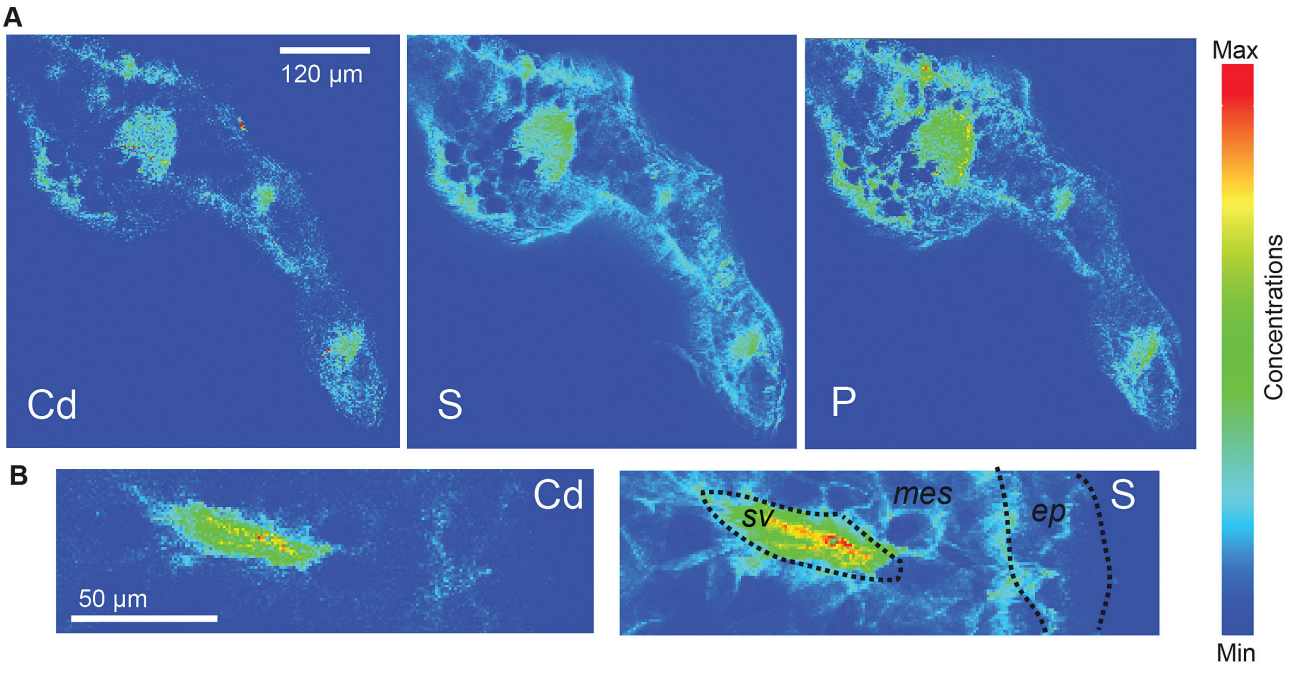

Fig. 6. Elemental µXRF maps of cryo cross-sections of *Arabidopsis lyrata* after 3 weeks Cd treatment (step size=4 µm, counting time=130 ms for A; step size=1 µm and counting time=500 ms for B). Cd is distributed in the vascular system as for *A. halleri* and also in the epidermis. The mesophyll seems less enriched than for the hyperaccumulator. (This figure is available in colour at *JXB* online.)

scale. However, correct spectra were obtained on *A. halleri* xylem and phloem as well as on *A. lyrata* phloem and epidermis. For both plants, phloem spectra were correctly reproduced by Cd–GSH only, while larger S-containing molecules (e.g. phytochelatins) were not tested. For *A. halleri* xylem, a good fit was obtained with 49% Cd–GSH+28% Cd–cell wall (NSS=4.64 10^{-4}). These results suggest that the Cd chemical species differ slightly in the phloem, where the metal is bound to thiol groups, and in the xylem, where it is mainly bound to S atoms but also to O atoms. The *A. lyrata* epidermis spectrum could be reproduced by 63% Cd–GSH+11% Cd–cell wall, indicating the dominance of thiol groups in Cd binding.

Discussion

Cd complexation in parents and progenies

Bulk XAS analyses showed that for the *A. halleri* accession used in this study, O atoms were the major ligands for Cd (60–70% and 80–90% after 1 and 3 weeks of Cd exposure, respectively). Shell fitting results were consistent with a higher proportion of O atoms, at 2.32±0.1 Å, than S atoms, at 2.52±0.1 Å. The sensitivity of Cd K-edge XAS for Cd organic complexes hardly allows the nature of O- and S-containing ligands to be clearly identified. O ligands may correspond to organic acids present in the vacuole and to polysaccharides of the cell wall. The high proportion of O ligands is consistent with previous results on Cd hyperaccumulators, namely *A. halleri* (Huguet *et al.*, 2012), *N. caerulescens* (Küpper *et al.*, 2004; Ueno *et al.*, 2005), or *N. praecox* (Vogel-Mikuš *et al.*, 2010; Koren *et al.*, 2013). A contrasting Cd speciation was observed in *A. lyrata*, in which Cd–S species represented 100% and 70% of Cd species after 1 and 3 weeks of exposure, respectively. These results are in line with a detoxification mechanism based on thiol ligands for non-tolerant non-hyperaccumulating plants, probably as phytochelatins and glutathione complexes as detailed in the Introduction. µXRF and µXANES results demonstrate that these Cd–S species are mainly concentrated in the epidermis and vascular bundles.

The higher proportion of Cd–S species observed at the shorter exposure time for both species suggests that the same two detoxification pathways exist in the two species, at different levels. Detoxification by thiol ligands appears first and remains dominant in *A. lyrata*, whereas it is always minor and decreases with time to the benefit of complexation by cell wall components and sequestration as Cd–organic acid complexes in the vacuole and/or efflux in the apoplast in *A. halleri*.

Results on progenies showed the exclusive presence of Cd–S species in sensitive plants. In contrast, tolerant progenies contained a mixture of Cd–O and Cd–S species. Therefore, these results highlight a link between Cd speciation and the tolerance trait. There was no correlation between Cd accumulation and Cd speciation. In contrast, in a study on Zn speciation in leaves of progenies from a F_2 cross between *A. halleri* and *A. lyrata*, a correlation was found between Zn speciation and Zn content—the link with Zn tolerance was not tested (Sarret *et al.*, 2009). The fact that Zn and Cd are handled differently in the leaves is not surprising. Their toxicity differs; Zn is essential and Cd is not, Zn levels in leaves are one to two orders of magnitude higher than Cd (so the metal/ligands ratio), and detoxification by thiol ligands does not operate for Zn, at least in a major way.

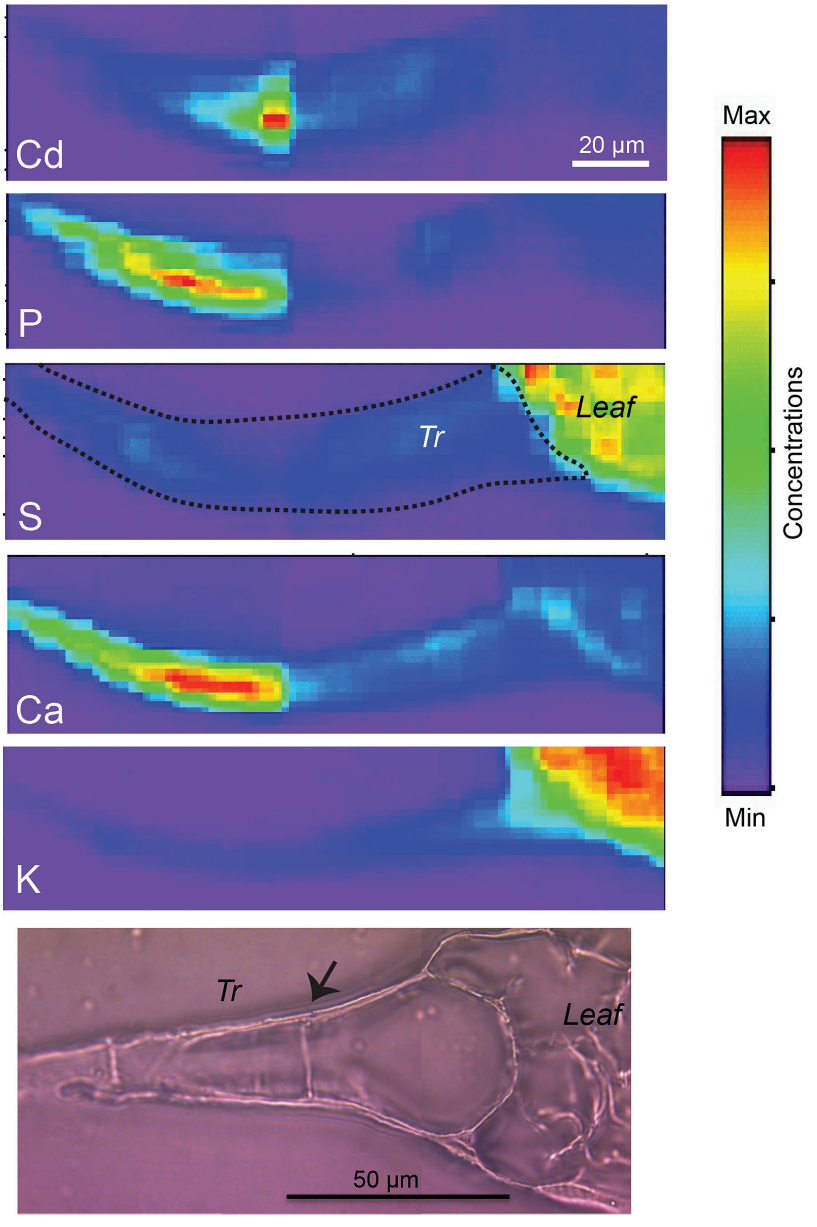

Fig. 7. Elemental µXRF maps of an *Arabidopsis halleri* trichome (E=3.57 keV for Cd, S, and P, and=4.10 keV for Ca and K, step size=2 µm, counting time=400 ms for Cd, S, and P, and 100 ms for Ca and K) and optical image of a 10 µm thick section trichome. Hot spots of Cd were found in a ring of the trichomes (Tr) probably associated with thickening of the cell wall (arrow). (This figure is available in colour at *JXB* online.)

Concerning the forms of transport of Cd, Cd–S was the dominant species in the three vascular tissues investigated by µXANES (phloem of *A. halleri* and *A. lyrata* and xylem of *A. halleri*) and minor O ligands were observed in *A. halleri* xylem. Thiol species were identified in the stem of *N. caerulescens* (Küpper *et al.*, 2004), whereas Ueno *et al.* (2008) suggested the presence of free Cd^{2+} in the xylem sap of *A. halleri*. Mendoza-Cózatl et al. (2008) also proposed that in the xylem of *B. napus*, Cd was not transported by thiol groups only and that other molecules containing oxygen or nitrogen ligands may be involved in the complexation of Cd. This corroborates the mixture of ligands identified in the present *A. halleri* xylem. The form of other metals in the xylem is also debated. Metals could be transported mainly as free cations, for instance Zn in *N. caerulescens* (Salt *et al.*, 1999) and *S. alfredii* (Lu *et al.*, 2013), or with histidine (Küpper *et al.*, 2004) as for Ni (Kerkeb and Krämer, 2003). While the complex of Zn with nicotianamine, a low-molecular non-proteinogenic amino acid, could form *in vivo* (Trampczynska *et al.*, 2010), and was identified in *A. halleri* roots (Deinlein *et al.*, 2012), a recent study ruled out its occurrence in *A. halleri* xylem and proposed that the metal rather formed coordination complexes with organic acids (Cornu *et al.*, 2015). To the authors' knowledge, the Cd–nicotianamine complex has not been identified so far. Furthermore, a higher sensitivity to Cd of *Arabidopsis* plants with deficient nicotianamine synthase 4 and enhanced tolerance to Cd of AtNAS4 overexpressors were proposed to be related to modified Fe homeostasis (Koen *et al.*, 2013). The authors proposed that by improving iron homeostasis, nicotianamine would reduce Cd toxicity

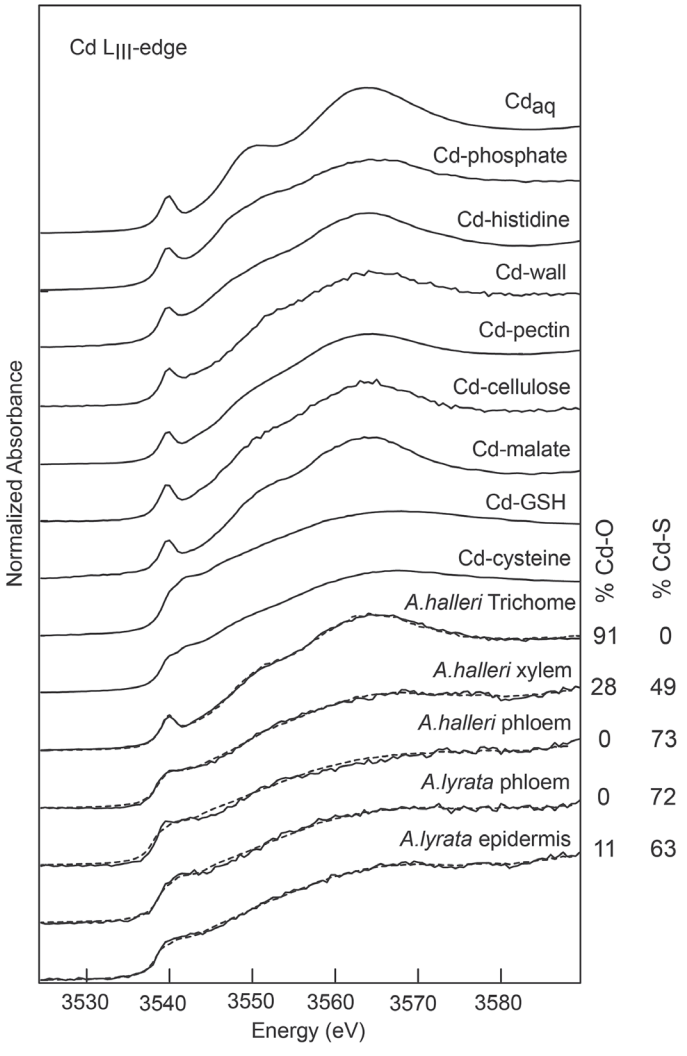

Fig. 8. Cd L_{III}-edge μXANES spectra for points of interest from 3 weeks 10 μM Cd treatment of *A. halleri* and *A. lyrata* maps compared with Cd model compounds. The dashed lines represent the best linear combination fits.

by limiting binding of Cd to metal (Fe)-binding molecules. There are fewer data concerning metals in the phloem, but transport of Cd by glutathione, and maybe by phytochelatins, has been proposed (Mendoza-Cózatl *et al.*, 2008, 2011). The Cd concentration was much higher in *B. napus* phloem than in the xylem, and the concentration of PCs+GSH together with the dissociation constants of Cd–cysteine (1.28×10^{-10} M), Cd–GSH (3.16×10^{-11} M), and Cd–PCs (7.9×10^{-17} M), and the more basic pH in the phloem than in the xylem supported the transport of Cd as Cd–PCs and Cd–GSH over a long-distance in the plant. Such a mode of transport may exist in both *A. halleri* and *A. lyrata* phloem. A higher content of glutathione and phytochelatins has also been found in the phloem of *Ricinus communis* in relation to As exposure (Ye *et al.*, 2010).

Cd compartmentalization in A. halleri *and* A. lyrata

Compartmentalization is known to be a way of detoxification in hyperaccumulators. In this work, distinct mechanisms of compartmentalization in *A. halleri* and in *A. lyrata* were highlighted.

For both species, high concentrations of Cd were located in the vascular system in the midrib and in secondary veins. The intensity of the Cd signal in veins was at the same level as in the leaf edge for *A. halleri*, whereas the Cd signal in veins was always higher than in other parts of *A. lyrata*. This observation can be explained by an increased unloading of the metal from veins to leaf tissue in the hyperaccumulator as observed for Zn in the same species (Sarret *et al.*, 2009), and as generally admitted. In the vascular system, the first and clear evidence of the presence of Cd in the phloem of *A. halleri* leaves is provided. It was more difficult to conclude for *A. lyrata* because of the lower resolution of the image and less intense signal. Phloem reallocation of Zn was evidenced in the Zn-hyperaccumulator *S. alfredii* by Lu *et al.* (2013) using stable isotope ^{68}Zn labelling. Cd was also identified in the root phloem of *A. thaliana* (Van Belleghem *et al.*, 2007), and phloem transport of Cd in rice was observed *in vivo* using ^{107}Cd (Fujimaki *et al.*, 2010). High amounts of Cd were also identified in *N. praecox* seeds (Vogel-Mikuš *et al.*, 2010), phloem, and collenchyma (Vogel-Mikuš et al., 2008b). In *N. caerulescens*, high expression of HMA4 was also observed in phloem vessels (Craciun *et al.*, 2012). These results suggest that some portion of metals is reallocated from mature leaves to younger leaves, seeds, or roots.

The present results also confirm previous observations (Küpper *et al.*, 2000; Zhao *et al.*, 2000) showing that Cd was more concentrated in the mesophyll than in the epidermis. In contrast, the epidermis of the non-accumulator *A. lyrata* showed a higher level of metal than the mesophyll. The edge of the leaves was also enriched with Cd in contrast to S and P, and this corroborates previous results on *A. halleri* (Huguet *et al.*, 2012) and *N. caerulescens* (Cosio *et al.*, 2005). At the cell level, Cd was found in the intracellular compartment, possibly in vacuoles, but the resolution did not allow conclusions to be reached on this point. Interestingly, the observations suggested an additional location of Cd at the cell rim, possibly in cell walls or the apoplast, supporting the idea that the extracellular compartment may play a role in Cd accumulation. Cell walls are well known to contribute to immobilization of toxic metal ions by binding them to acidic pectins, histidyl groups, and negatively charged cellulose, or by constituting a barrier to metal uptake into the cytosol (Krzesłowska, 2011). Significant amounts, although not the majority, of Cd were observed in the apoplast and/or cell walls of *N. caerulescens* (Cosio *et al.*, 2005). Interestingly, the capacity for Cd hyperaccumulation in some populations of *N. caerulescens* (such as Ganges) exceeds that of all *A. halleri* populations analysed up to now. In the Prayon ecotype, 23% of Cd was modelled as complexed with the cell walls, whereas in the Ganges ecotype Cd–cell wall complexes were absent (Ebbs *et al.*, 2009). It should also be noted that up to now no vacuolar transporter of Cd was clearly identified in *A. halleri*. While the role of HMA3 in the high Cd vacuolar sequestration capacity of *N. caerulescens* is well established, AhHMA3 does not seem to transport Cd (but transports Zn well) as deduced from heterologous expression in *Saccharomyces*

cerevisiae (Becher *et al.* 2004). Furthermore, the MTP1 transporter, involved in vacuolar Zn^{2+} sequestration in *A. halleri*, was shown to have higher selectivity for Zn than Cd (Kawachi *et al.*, 2012) and was not identified in QTL analysis investigating Cd tolerance, in contrast to studies on Zn tolerance (Courbot *et al.*, 2007).

Finally, trichomes of both *A. halleri* and *A. lyrata* contained Cd hot spots delimiting the P- and Ca-enriched upper part of the cell. µXANES identified oxygen ligands for Cd in the trichomes, as already observed for *A. thaliana* (Isaure *et al.*, 2006). Thus, this sequestration is not specific to hyperaccumulators. Although intense Cd concentrations are present, these very localized and small hot spots represent a minor part of Cd storage in the shoots, as described for Zn in Sarret *et al.* (2009).

To conclude, this study showed complex responses of *A. halleri* and *A. lyrata* to Cd exposure. The same detoxification mechanisms, namely chelation by thiol ligands, vacuolar sequestration, and possibly efflux in the apoplast, seemed to be used in the two species but at very different levels. Chelation by S ligands was the major mechanism in *A. lyrata*. In *A. halleri*, intracellular (probably vacuolar) sequestration but also possibly efflux in the apoplast, both associated with binding with O ligands, dominated. In both species, the extent of chelation by S ligands decreased with exposure time. The study of Cd speciation in progenies showed that the chemical form of Cd was linked to the Cd tolerance trait. Evidence of Cd transport through the phloem, suggesting some re-allocation processes, was provided. In both xylem and phloem of *A. halleri* and xylem of *A. lyrata*, Cd speciation was dominated by Cd–S species. Finally, this study shows that it is of interest to combine imaging and spectroscopic techniques with a submicron resolution with bulk analyses to obtain a global view of metals status in biological samples.

Supplementary data

Supplementary data are available at *JXB* online.

Figure S1. Cd K-edge XANES spectra of *A. lyrata* and *A. halleri* shown with various linear combination fits.

Table S1. Composition of the modified Murashige and Skoog solution and culture conditions.

Table S2. Summary of analyses performed.

Acknowledgements

This work was supported by PHYMET ANR project no. 2010 JCJC 605 01 and the Belgian National Fund for Scientific Research FNRS-PDR T.0206.13. We also thank the ESRF (Grenoble, France) and Soleil (Saclay, France) for the provision of beamtime. ISTerre is part of Labex OSUG@2020 (ANR10 LABX56).

References

Assuncao AGL, Martins PD, De Folter S, Vooijs R, Schat H, Aarts MGM. 2001. Elevated expression of metal transporter genes in three accessions of the metal hyperaccumulator Thlaspi caerulescens. *Plant, Cell and Environment* **24,** 217–226.

Baker AJM, Brooks RR. 1989. Terrestrial higher plants which hyperaccumulate metallic elements. A review of their distribution, ecology and phytochemistry. *Biorecovery* **1,** 81–126.

Baker AJM, Reeves RD, Hajar ASM. 1994. Heavy metal accumulation and tolerance in British populations of the metallophyte Thlaspi caerulescens J.& C.Presl (Brassicaceae). *New Phytologist* **127,** 61–68.

Becher M, Talke IN, Krall L, Krämer U. 2004. Cross-species microarray transcript profiling reveals high constitutive expression of metal homeostasis genes in shoots of the zinc hyperaccumulator Arabidopsis halleri. *The Plant Journal* **37,** 251–268.

Bert V, Bonnin I, Saumitou-Laprade P, De Laguerie P, Petit D. 2002. Do Arabidopsis halleri from nonmetallicolous populations accumulate zinc and cadmium more effectively than those from metallicolous populations? *New Phytologist* **155,** 47–57.

Bert V, Meerts P, Saumitou-Laprade P, Salis P, Gruber W, Verbruggen N. 2003. Genetic basis of Cd tolerance and hyperaccumulation in Arabidopsis halleri. *Plant and Soil* **249,** 9–18.

Carrier P, Baryla A, Havaux M. 2003. Cadmium distribution and microlocalization in oilseed rape (Brassica napus) after long-term growth on cadmium-contaminated soil. *Planta* **216,** 939–950.

Chardonnens AN, tenBookum WM, Kuijper LDJ, Verkleij JAC, Ernst WHO. 1998. Distribution of cadmium in leaves of cadmium tolerant and sensitive ecotypes of Silene vulgaris. *Physiologia Plantarum* **104,** 75–80.

Clemens S. 2001. Molecular mechanisms of plant metal tolerance and homeostasis. *Planta* **212,** 475–486.

Clemens S, Aarts MGM, Thomine S, Verbruggen N. 2013. Plant science: the key to preventing slow cadmium poisoning. *Trends in Plant Science* **18,** 92–99.

Clemens S, Simm C. 2003. *Schizosaccharomyces pombe* as a model for metal homeostasis in plant cells: the phytochelatin-dependent pathway is the main cadmium detoxification mechanism. *New Phytologist* **159,** 323–330.

Cobbett C, Goldsbrough P. 2002. Phytochelatins and metallothioneins: roles in heavy metal detoxification and homeostasis. *Annual Review of Plant Biology* **53,** 159–182.

Cornu JY, Deinlein U, Höreth S, Braun M, Schmidt H, Weber M, Persson DP, Husted S, Schjoerring JK, Clemens S. 2015. Contrasting effects of nicotianamine synthase knockdown on zinc and nickel tolerance and accumulation in the zinc/cadmium hyperaccumulator Arabidopsis halleri. *New Phytologist* **206,** 738–50.

Cosio C, DeSantis L, Frey B, Diallo S, Keller C. 2005. Distribution of cadmium in leaves of Thlaspi caerulescens. *Journal of Experimental Botany* **56,** 765–775.

Courbot M, Willems G, Motte P, Arvidsson S, Roosens N, Saumitou-Laprade P, Verbruggen N. 2007. A major quantitative trait locus for cadmium tolerance in Arabidopsis halleri colocalizes with HMA4, a gene encoding a heavy metal ATPase. *Plant Physiology* **144,** 1052–1065.

Craciun AR, Meyer CL, Chen J, Roosens N, De Groodt R, Hilson P, Verbruggen N. 2012. Variation in HMA4 gene copy number and expression among Noccaea caerulescens populations presenting different levels of Cd tolerance and accumulation. *Journal of Experimental Botany* **63,** 4179–4189.

Deinlein U, Weber M, Schmidt H, *et al*. 2012. Elevated nicotianamine levels in *Arabidopsis halleri* roots play a key role in zinc hyperaccumulation. *The Plant Cell* **24,** 708–723.

Dräger DB, Desbrosses Fonrouge AG, Krach C, Chardonnens AN, Meyer RC, Saumitou Laprade P, Krämer U. 2004. Two genes encoding Arabidopsis halleri MTP1 metal transport proteins co-segregate with zinc tolerance and account for high MTP1 transcript levels. *The Plant Journal* **39,** 425–439.

Ebbs S, Lau I, Ahner B, Kochian L. 2002. Phytochelatin synthesis is not responsible for Cd tolerance in the Zn/Cd hyperaccumulator Thlaspi caerulescenes (J. and C. Presl). *Planta* **214,** 635–640.

Ebbs SD, Zambrano MC, Spiller SM, Newville M. 2009. Cadmium sorption, influx, and efflux at the mesophyll layer of leaves from ecotypes of the Zn/Cd hyperaccumulator Thlaspi caerulescens. *New Phytologist* **181,** 626–636.

Fujimaki S, Suzui N, Ishioka NS, Kawachi N, Ito S, Chino M, Nakamura S. 2010. Tracing cadmium from culture to spikelet: noninvasive imaging and quantitative characterization of absorption, transport, and

accumulation of cadmium in an intact rice plant. *Plant Physiology* **152,** 1796–1806.

Fukuda N, Hokura A, Kitajima N, Terada Y, Saito H, Abe T, Nakai I. 2008. Micro X-ray fluorescence imaging and micro X-ray absorption spectroscopy of cadmium hyper-accumulating plant, Arabidopsis halleri ssp. gemmifera, using high-energy synchrotron radiation. *Journal of Analytical Atomic Spectrometry* **23,** 1068–1075.

Hanikenne M, Talke IN, Haydon MJ, Lanz C, Nolte A, Motte P, Kroymann J, Weigel D, Krämer U. 2008. Evolution of metal hyperaccumulation required cis-regulatory changes and triplication of HMA4. *Nature* **453,** 391–395.

Huguet S, Bert V, Laboudigue A, Barthès V, Isaure MP, Llorens I, Schat H, Sarret G. 2012. Cd speciation and localization in the hyperaccumulator Arabidopsis halleri. *Environmental and Experimental Botany* **82,** 54–65.

Isaure MP, Fayard B, Sarret G, Pairis S, Bourguignon J. 2006. Localization and chemical forms of cadmium in plant samples by combining analytical electron microscopy and X-ray spectromicroscopy. Spectrochimica Acta. *Part B Atomic Spectroscopy* **61,** 1242–1252.

Isaure MP, Sarret G, Harada E, *et al*. 2010. Calcium promotes cadmium elimination as vaterite grains by tobacco trichomes. *Geochimica et Cosmochimica Acta* **74,** 5817–5834.

Kawachi M, Kobae Y, Kogawa S, Mimura T, Krämer U, Maeshima M. 2012. Amino acid screening based on structural modeling identifies critical residues for the function, ion selectivity and structure of Aradidopsis MTP1. *FEBS Journal* **279,** 2339–2356.

Kerkeb L, Krämer U. 2003. The role of free histidine in xylem loading of nickel in Alyssum lesbiacum and Brassica juncea. *Plant Physiology* **131,** 716–724.

Koen E, Besson-Bard A, Duc C, Astier J, Gravot A, Richaud P, Lamotte O, Boucherez J, Gaymard F, Wendehenne D. 2013. Arabidopsis thaliana nicotianamine synthase 4 is required for proper response to iron deficiency and to cadmium exposure. *Plant Science* **209,** 1–11.

Koji N, Yuichi Y, Ryumon H, Masao I, Ikiko T, Shunichi K, Takashi K. 1983. The relationship between itai-itai disease among inhabitants of the jinzu river basin and cadmium in rice. *Toxicology Letters* **17,** 263–266.

Koren S, Arčon I, Kump P, Nečemer M, Vogel-Mikuš K. 2013. Influence of CdCl2 and CdSO4 supplementation on Cd distribution and ligand environment in leaves of the Cd hyperaccumulator Noccaea (Thlaspi) praecox. *Plant and Soil* **370,** 125–148.

Krämer U. 2010. Metal hyperaccumulation in plants. *Annual Review of Plant Biology* **61,** 517–534.

Krzesłowska M. 2011. The cell wall in plant cell response to trace metals: polysaccharide remodeling and its role in defense strategy. *Acta Physiologia Plantarum* **33,** 35–51.

Küpper H, Kochian LV. 2010. Transcriptional regulation of metal transport genes and mineral nutrition during acclimatization to cadmium and zinc in the Cd/Zn hyperaccumulator, Thlaspi caerulescens (Ganges population). *New Phytologist* **185,** 114–129.

Küpper H, Lombi E, Zhao FJ, McGrath SP. 2000. Cellular compartmentation of cadmium and zinc in relation to other elements in the hyperaccumulator Arabidopsis halleri. *Planta* **212,** 75–84.

Küpper H, Mijovilovich A, Meyer-Klaucke W, Kroneck PMH. 2004. Tissue-and age-dependent differences in the complexation of cadmium and zinc in the cadmium/zinc hyperaccumulator Thlaspi caerulescens (Ganges ecotype) revealed by X-ray absorption spectroscopy. *Plant Physiology* **134,** 748–757.

Lane TW, Morel FMM. 2000. A biological function for cadmium in marine diatoms. *Proceedings of the National Academy of Sciences, USA* **97,** 4627–4631.

Leitenmaier B, Küpper H. 2011. Cadmium uptake and sequestration kinetics in individual leaf cell protoplasts of the Cd/Zn hyperaccumulator Thlaspi caerulescens. *Plant, Cell and Environment* **34,** 208–219.

Liu W, Shu W, Lan C. 2004. Viola baoshanensis, a plant that hyperaccumulates cadmium. *Chinese Science Bulletin* **49,** 29–32.

Liu X, Peng K, Wang A, Lian C, Shen Z. 2010. Cadmium accumulation and distribution in populations of Phytolacca americana L. and the role of transpiration. *Chemosphere* **78,** 1136–1141.

Lu L, Tian S, Zhang J, Yang X, Labavitch JM, Webb SM, Latimer M, Brown PH. 2013. Efficient xylem transport and phloem remobilization of Zn in the hyperaccumulator plant species Sedum alfredii. *New Phytologist* **198,** 721–731.

Ma JF, Ueno D, Zhao FJ, McGrath SP. 2005. Subcellular localisation of Cd and Zn in the leaves of a Cd-hyperaccumulating ecotype of Thlaspi caerulescens. *Planta* **220,** 731–736.

Macnair MR, Bert V, Huitson SB, Saumitou-Laprade P, Petit D. 1999. Zinc tolerance and hyperaccumulation are genetically independent characters. *Proceedings of the Royal Society B: Biological Sciences* **266,** 2175–2179.

McLaughlin MJ, Singh BR. 1999. Cadmium in soils and plants. In: McLaughlin MJ, Singh BR, eds. *Cadmium in soils and plants*. Dordrecht: Kluwer Academic Publishers, 1–9.

Mendoza-Cózatl DG, Butko E, Springer F, Torpey JW, Komives EA, Kehr J, Schroeder JI. 2008. Identification of high levels of phytochelatins, glutathione and cadmium in the phloem sap of Brassica napus. A role for thiol-peptides in the long-distance transport of cadmium and the effect of cadmium on iron translocation. *The Plant Journal* **54,** 249–259.

Mendoza-Cózatl DG, Jobe TO, Hauser F, Schroeder JI. 2011. Long-distance transport, vacuolar sequestration, tolerance, and transcriptional responses induced by cadmium and arsenic. *Current Opinion in Plant Biology* **14,** 554–562.

Meyer CL, Verbruggen N. 2012. The use of the model species Arabidopsis halleri towards phytoextraction of cadmium polluted soils. *New Biotechnology* **30,** 9–14.

Ó Lochlainn S, Bowen HC, Fray RG, Hammond JP, King GJ, White PJ, Graham NS, Broadley MR. 2011. Tandem quadruplication of HMA4 in the zinc (Zn) and cadmium (Cd) hyperaccumulator Noccaea caerulescens. *PLoS One* **6,** e17814.

Park J, Song WY, Ko D, Eom Y, Hansen TH, Schiller M, Lee TG, Martinoia E, Lee Y. 2012. The phytochelatin transporters AtABCC1 and AtABCC2 mediate tolerance to cadmium and mercury. *The Plant Journal* **69,** 278–288.

Perronnet K, Schwartz C, Morel JL. 2003. Distribution of cadmium and zinc in the hyperaccumulator Thlaspi caerulescens grown on multicontaminated soil: distribution of metals in Thlaspi caerulescens. *Plant and Soil* **249,** 19–25.

Ravel B, Newville M. 2005. ATHENA, ARTEMIS, HEPHAESTUS: data analysis for X-ray absorption spectroscopy using IFEFFIT. *Journal of Synchrotron Radiation* **12,** 537–541.

Roosens NHCJ, Willems G, Saumitou-Laprade P. 2008. Using Arabidopsis to explore zinc tolerance and hyperaccumulation. *Trends in Plant Science* **13,** 208–215.

Salt DE, Prince RC, Baker AM, Raskin I, Pickering IJ. 1999. Zinc ligands in the metal hyperaccumulator *Thlaspi caerulescens* as determined using X-ray absorption absorption spectroscopy. *Environmental Science and Technology* **33,** 713–717.

Salt DE, Prince RC, Pickering IJ, Raskin I. 1995. Mechanisms of cadmium mobility and accumulation in indian mustard. *Plant Physiology* **109,** 1427–1433.

Sarret G, Smits EAHP, Michel HC, Isaure MP, Zhao FJ, Tappero R. 2013. Use of synchrotron-based techniques to elucidate metal uptake and metabolism in plants. *Advances in Agronomy* **119,** 1–82.

Sarret G, Willems G, Isaure MP, Marcus MA, Fakra SC, Frérot H, Pairis S, Geoffroy N, Manceau A, Saumitou-Laprade P. 2009. Zinc distribution and speciation in Arabidopsis halleri × Arabidopsis lyrata progenies presenting various zinc accumulation capacities. *New Phytologist* **184,** 581–595.

Schat H, Llugany M, Vooijs R, Hartley Whitaker J, Bleeker PM. 2002. The role of phytochelatins in constitutive and adaptative heavy metal tolerances in hyperaccumulator and non-hyperaccumulator metallophytes. *Journal of Experimental Botany* **53,** 2381–2392.

Shahzad Z, Gosti F, Frérot H, Lacombe E, Roosens N, Saumitou-Laprade P, Berthomieu P. 2010. The five AHMTP1 zinc transporters undergo different evolutionary fates towards adaptive evolution to zinc tolerance in Arabidopsis halleri. *PLoS Genetics* **6,** e1000911.

Song WY, Mendoza-Cózatl DG, Lee Y, Schroeder JI, Ahn SN, Lee HS, Wicker T, Martinoia E. 2013. Phytochelatin-metal(loid) transport into vacuoles shows different substrate preferences in barley and Arabidopsis. *Plant, Cell and Environment* **37,** 1192–1201.

Sun Q, Ye ZH, Wang XR, Wong MH. 2007. Cadmium hyperaccumulation leads to an increase of glutathione rather than phytochelatins in the cadmium hyperaccumulator Sedum alfredii. *Journal of Plant Physiology* **164,** 1489–1498.

Tang YT, Qiu RL, Zeng XW, Fang X, Yu FM, Zhou XY, Wu Y. 2009*b*. Zn and Cd hyperaccumulating characteristics of Picris divaricata vant. *International Journal of Environment and Pollution* **38,** 26–38.

Tang YT, Qiu RL, Zeng XW, Ying RR, Yu FM, Zhou XY. 2009*a*. Lead, zinc, cadmium hyperaccumulation and growth stimulation in Arabis paniculata Franch. *Environmental and Experimental Botany* **66,** 126–134.

Tian S, Lu L, Labavitch J, Yang X, He Z, Hu H, Sarangi R, Newville M, Commisso J, Brown P. 2011. Cellular sequestration of cadmium in the hyperaccumulator plant species Sedum alfredii. *Plant Physiology* **157,** 1914–1925.

Trampczynska A, Küpper H, Meyer-Klaucke W, Schmidt H, Clemens S. 2010. Nicotianamine forms complexes with Zn(ii) *in vivo*. *Metallomics* **2,** 57–66.

Ueno D, Ma JF, Iwashita T, Zhao FJ, McGrath SP. 2005. Identification of the form of Cd in the leaves of a superior Cd-accumulating ecotype of Thlaspi caerulescens using Cd-113-NMR. *Planta* **221,** 928–936.

Ueno D, Milner MJ, Yamaji N, Yokosho K, Koyama E, Clemencia Zambrano M, Kaskie M, Ebbs S, Kochian LV, Ma JF. 2011. Elevated expression of TcHMA3 plays a key role in the extreme Cd tolerance in a Cd-hyperaccumulating ecotype of Thlaspi caerulescens. *The Plant Journal* **66,** 852–862.

Van Belleghem F, Cuypers A, Semane B, Smeets K, Vangronsveld J, D'Haen J, Valcke R. 2007. Subcellular localization of cadmium in roots and leaves of Arabidopsis thaliana. *New Phytologist* **173,** 495–508.

Verbruggen N, Hermans C, Schat H. 2009. Molecular mechanisms of metal hyperaccumulation in plants. *New Phytologist* **181,** 759–776.

Vogel-Mikuš K, Arčon I, Kodre A. 2010. Complexation of cadmium in seeds and vegetative tissues of the cadmium hyperaccumulator Thlaspi praecox as studied by X-ray absorption spectroscopy. *Plant and Soil* **331,** 439–451.

Vogel-Mikuš K, Regvar M, Mesjasz-Przybyłowicz J, Przybyłowicz WJ, Simčič J, Pelicon P, Budnar M. 2008*a*. Spatial distribution of cadmium in leaves of metal hyperaccumulating Thlaspi praecox using micro-PIXE. *New Phytologist* **179,** 712–721.

Vogel-Mikuš K, Simčič J, Pelicon P, Budnar M, Kump P, Nečemer M, Mesjasz-Przybyłowicz J, Przybyłowicz WJ, Regvar M. 2008*b*. Comparison of essential and non-essential element distribution in leaves of the Cd/Zn hyperaccumulator Thlaspi praecox as revealed by micro-PIXE. *Plant, Cell and Environment* **31,** 1484–1496.

Wang SL, Liao WB, Yu FQ, Liao B, Shu WS. 2009. Hyperaccumulation of lead, zinc, and cadmium in plants growing on a lead/zinc outcrop in Yunnan Province, China. *Environmental Geology* **58,** 471–476.

Willems G, Drager DB, Courbot M, Godé C, Verbruggen N, Saumitou-Laprade P. 2007. The genetic basis of zinc tolerance in the metallophyte Arabidopsis halleri ssp. halleri (Brassicaceae): an analysis of quantitative trait loci. *Genetics* **176,** 659–674.

Willems G, Frérot H, Gennen J, Salis P, Saumitou-Laprade P, Verbruggen N. 2010. Quantitative trait loci analysis of mineral element concentrations in an Arabidopsis halleri × Arabidopsis lyrata petraea F2 progeny grown on cadmium-contaminated soil. *New Phytologist* **187,** 368–379.

Wójcik M, Vangronsveld J, D'Haen J, Tukiendorf A. 2005. Cadmium tolerance in Thlaspi caerulescens: II. Localization of cadmium in Thlaspi caerulescens. *Environmental and Experimental Botany* **53,** 163–171.

Yang X, Li T, Yang J, He Z, Lu L, Meng F. 2006. Zinc compartmentation in root, transport into xylem, and absorption into leaf cells in the hyperaccumulating species of Sedum alfredii Hance. *Planta* **224,** 185–195.

Ye WL, Wood BA, Stroud JL, Andralojc PJ, Raab A, McGrath SP, Feldmann J, Zhao FJ. 2010. Arsenic speciation in phloem and xylem exudates of castor bean. *Plant Physiology* **154,** 1505–1513.

Zhao FJ, Lombi E, Breedon T, McGrath SP. 2000. Zinc hyperaccumulation and cellular distribution in Arabidopsis halleri. *Plant, Cell and Environment* **23,** 507–514.